

POLITECNICO DI TORINO

Department of Electronics and Telecommunication (DET)



**Politecnico
di Torino**

Master Degree Course

**Cloaking of large implanted metallic structures in human
body using magnetic materials**

Communications and Computer Networks Engineering

Candidate: Muhammad Raashid

Supervisor: Ladislau Matekovits

Co-supervisor: Ildiko Peter

December 2021

Abstract:

Biomedical implants are used in case of damaged bones and tissues to restore physiological functions in the human body. For this purpose, many metals such as titanium alloys are used as implants which are then covered with another material for biocompatibility to avoid corrosion and side effects of metal components. When subjected to electromagnetic waves, it gives a particular electromagnetic response that is very different from a human bone, making it detectable through metal detectors and other equipment. We only want to simulate the same response as in a bone structure when these implants are subjected inside the human bone.

Cloaking is a technology that makes different materials partially or fully invisible to the electromagnetic spectrum or for particular frequencies. To cloak these implants usually periodic materials are used to cover these materials to have the same response as in the case of a bone. However, periodic materials, when used for a flat surface, are easy to design and manufacture. As cylindrical or conical implants have to be inserted in a bone to support broken bone, cloaking with these periodic materials becomes difficult as these flat surfaces need to be bent and joined at the end. These structures undergo different stress on the outer and inner radii. Thus, we do not get a uniform response throughout the geometry, usually when joined or bent.

To solve this issue, we have used magnetic materials to avoid periodic materials and design complexity. Firstly, the response of a human bone with the respective muscle, fat, and skin covering is studied. Then, the implant alone with a dielectric inserted, and the response obtained. Thus the deviation between these two responses is reduced by covering the implant and dielectric with magnetic material to get the same response as the bone structure. Then biocompatibility is obtained by covering this structure with a bio-compatible material inside the bone. Finally, the simulations are repeated with different permeability's to check for the response for other magnetic materials.

Acknowledgments

Performing graduation projects and writing this thesis has been a long journey. It would not have been possible without the support and motivation of a few individuals whom I would like to acknowledge.

I want to express my sincere gratitude to my supervisor Professor Ladislau Matekovits at Politecnico di Torino for his valuable help, guidance, and continuous support throughout the project. Finally, I owe a great deal to my entire family, especially my dear father, mother, and wife, who always supported me throughout my life.

Contents

Chapter 1	7
1. Introduction	7
Chapter 2	9
2. Literature Review	9
2.1 Permeability.....	9
2.2 Magnetic Field and Magnetic field Density	9
2.3 Hysteresis.....	10
2.4 Diamagnetism.....	10
2.5 Paramagnetism.....	10
2.6 Radar Cross-section.....	11
Chapter 3	12
3. Simulations and Results	12
3.1 Geometry	12
3.2 Methodology.....	13
3.3 Case 1: Bone, Muscle, Fat and Skin.....	15
3.4 Case 2: Implant, Bone, Muscle, Fat, and Skin	19
3.5 Case 3: Implant, Dielectric, Bone, Muscle, Fat, and Skin.....	22
3.6 Case 4: Implant, Dielectric, Magnetic material, Surface Impedance, Bone, Muscle, Fat, and Skin	26
3.7 Case 5: Implant, Dielectric, Magnetic material, Surface Impedance, Bone, Muscle, Fat, and Skin.....	29
Chapter 4	32
4. Conclusion	32
4.1. Absolute Percentage Error.....	32
4.2. Relative Radar Cross-Section.....	33
4.3 Testing the structure for other values of magnetic permeability	33
References	35

List of figures

Figure 1: X-ray of a metal implant in human bone [1]	7
Figure 2: Example of a hysteresis loop	10
Figure 3: Overview of the complete geometry	12
Figure 4: Curve placement inside the bone	13
Figure 5: Scenario for the simulation	14
Figure 6: Geometry of only bone structure (case 01)	15
Figure 7: Electric Field Intensity in only bone structure at 2.4 GHz	16
Figure 8: Electric Field Intensity in only bone structure at 2.45 GHz	17
Figure 9: Electric Field Intensity in only bone structure at 2.5 GHz	17
Figure 10: Comparison of Electric Field Intensities at the three frequencies (Case 01)	18
Figure 11: Geometry of bone with implant structure (case 02)	19
Figure 12: Electric Field Intensity for Bone with Implant at 2.4 GHz	20
Figure 13: Electric Field Intensity for Bone with Implant at 2.45 GHz	20
Figure 14: Electric Field Intensity for Bone with Implant at 2.5 GHz	21
Figure 15: Comparison of Electric Field Intensities at the three frequencies (Case 02)	21
Figure 16: Geometry of Bone, Implant and Dielectric	22
Figure 17: Electric Field Intensity for Bone, Implant and Dielectric at 2.4 GHz	23
Figure 18: Electric Field Intensity for Bone, Implant and Dielectric at 2.45 GHz	23
Figure 19: Electric Field Intensity for Bone, Implant and Dielectric at 2.5 GHz	24
Figure 20: Comparison of Electric Field Intensities of the three frequencies (Case 03)	24
Figure 21: Comparison among Electric Field Intensities of case 01, 02 and 03 at 2.45 GHz	25
Figure 22: Geometry of the structure after adding surface impedance on the dielectric layer	26
Figure 23: Surface Impedance added to Dielectric Layer of $-j10$ Ohm at the three frequencies	27
Figure 24: Surface Imp added to Dielectric Layer of $-j480$ Ohm at the three frequencies	28
Figure 25: Comparison of only bone case with the surface impedance of -480 Ohm	28
Figure 26: Geometry of the final structure with magnetic material	29
Figure 27: Electric Field Intensity for the final structure with magnetic material at 2.4 GHz	30
Figure 28: Electric Field Intensity for the final structure with magnetic material at 2.45 GHz	30
Figure 29: Electric Field Intensity for the final structure with magnetic material at 2.5 GHz	31
Figure 30: Comparison of all the cases at 2.45 GHz	31
Figure 31: Comparison of Percentage Errors between implant and magnetic material cases	32
Figure 32: RCS computation for all the cases	33
Figure 33: Electric Field Intensities for different values of μ	34
Figure 34: Percentage Errors for different values of μ	34

List of Tables

Table 1: List of layers and their parameters for case 01	15
Table 2: List of layers and their parameters for case 02	19
Table 3: List of layers and their parameters for case 03	22
Table 4: List of layers and their parameters for case 04	26
Table 5: List of layers and their parameters for case 05	29

Chapter 1

1. Introduction

Metallic implants are frequently used in surgery to support and replace degenerated tissues. Because of its resistance to corrosion by human fluids, titanium is considered as the most biocompatible metal, with no detrimental or toxic effects on human tissue. The protective titanium oxide film provides this ability to endure the hostile body environment.



Figure 1: X-ray of a metal implant in human bone [1]

Metal implants in the body, such as joint replacements, plates, screws, and rods can trigger metal detectors during security screenings at airports. Patients were handed certificates by their doctors for many years, informing security officials about their implanted metal. But now, even with these documents, they have to go through second-tier checks to prove the contents of the certificates if they are true or not.

There was a need to change the electromagnetic properties of these implants to behave like normal bones to reduce the hassle at these checkpoints through metal detectors. When these implants are exposed to electromagnetic waves, they give a different electromagnetic response which is usually a change in the electromagnetic field detected by these metal detectors.

Cloaking has been introduced in these bone implants to avoid this problem. Cloaking is a technology that makes different materials partially or fully invisible to the electromagnetic spectrum or for particular frequencies. It reduces the scattering of electromagnetic waves and brings them down to the required levels—there are many techniques already in practice to acquire the cloaking effect. The most used technique is the use of metamaterials.

Metamaterials are defined as the designing of artificial structural elements in a way to make them of more advantage and confer additional electromagnetic properties. An electromagnetic material must possess specific properties such as permittivity and permeability, in a particular range of wavelength of electromagnetic radiation. For this, the material must be homogenous at that particular wavelength, implying that the molecule's size and spacing should be smaller than the wavelength. For example, if we are working with the microwave frequency range, where the wavelength is in order of centimeters, the size of the molecule should be in order of millimeters. This can be designed using the everyday common materials made up of molecules at this wavelength scale.

Metamaterials can be designed to achieve the scattering cancelation technique. For a long time, it has been recognized that scattering from an object can be reduced by introducing another object into the system whose scattering is complementary to that of the significant scattering object. This form of scattering minimization can be achieved by using single or many layers of dielectric materials to cover the main scattering item.

Some design complexities are involved in designing these metamaterials, making it very difficult to achieve cloaking for the cylindrical or conical implants in the human body. Metamaterials for flat surfaces are easy, but when these materials are designed for cylindrical or conical surfaces, it has some design limitations. When these flat materials are bent to cover the cylindrical geometries, there is a different amount of stress on the outer and inner radii, making the structure non-uniform. Thus, this non-uniformity causes many issues when exposed to electromagnetic waves as they exhibit different intensities throughout the width at the same point.

So, there is a need to explore new avenues for the cloaking of cylindrical or conical surfaces. The use of magnetic materials has not been explored a lot for cloaking. The magnetic materials with different electromagnetic properties such as permeability, permittivity, and conductance need to be studied to use for further research on whether they can be used for cloaking or not.

This thesis is based on the fact that the feasibility of magnetic material has been simulated in the software CST. The electromagnetic field of a bone with implant and magnetic material has been simulated. The comparison is made by further optimizing the widths of the magnetic materials to achieve the best-case scenario for cloaking. A lab-based piezoelectric material has been used in this study [3]. Furthermore, some random value of magnetic materials has been investigated for the possible cloaking effect.

Chapter 2

2. Literature Review

In this chapter, we discuss a few concepts related to electromagnetism which are used later on.

2.1 Permeability

The amount of magnetization a material acquires in response to an applied magnetic field is known as permeability. It is denoted by a Greek letter μ .

In SI units, permeability is measured in henry per meter (H/m) or newton per ampere squared (N/A²).

When magnetic field produced in a vacuum, the permeability constant μ_0 is the ratio between magnetic induction and magnetizing force.

Relative permeability is given by μ_r , and it is the ratio of the permeability of a medium to the permeability of vacuum (μ_0):

$$\mu_r = \frac{\mu}{\mu_0}$$

Where $4\pi \times 10^{-7}$ H/m is the magnetic permeability of free space.

2.2 Magnetic Field and Magnetic field Density

- The magnetic field H is produced by electric currents and displacement currents at the poles of magnets. The unit of H is amperes per meter in SI units.
- The magnetic flux density B causes electromagnetic induction by curving the motion of charges in the electrical domain. B is measured in volt-seconds/square meters in SI units (tesla).

There is a simple relationship between H and B in many materials (and in vacuum), at any location or time, in that the two fields are precisely proportional to each other:

$$\mathbf{B} = \mu \mathbf{H}$$

2.3 Hysteresis

The magnetic induction \mathbf{B} is out of phase with the magnetic driving force \mathbf{H} in this ferromagnetic phenomenon.

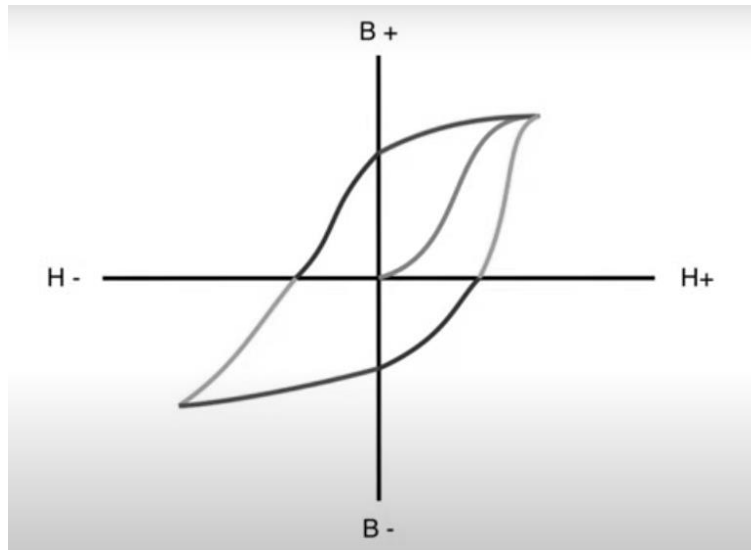


Figure 2: Example of a hysteresis loop

From the hysteresis loop, we can calculate permeability by taking a point on the hysteresis curve and dividing the projection of the curve on the y-axis, which is B , with the projection of the curve on the x-axis, which is H .

2.4 Diamagnetism

It is a property of an object that causes it to generate a magnetic field in opposition to an externally applied magnetic field, resulting in a repellent effect. An external magnetic field, in particular, changes the orbital velocity of electrons around their nuclei, causing the magnetic dipole moment to change in the opposite direction of the external field. Materials with a magnetic permeability of less than 0 are known as diamagnets.

2.5 Paramagnetism

It is a type of magnetism that only exists when a magnetic field is provided outside. Magnetic fields attract paramagnetic materials, resulting in a relative magnetic permeability larger than one.

2.6 Radar Cross-section

The radar cross-section (RCS) is a critical parameter that describes the electromagnetic wave-target object interaction. It also gives the measure of scattering when two structures are compared. The formula is given below:

$$RCS_{db} = 10 \log_{10} \left[2\pi r \left(\frac{|E_{implant}|^2 - |E_{ref}|^2}{|E_{ref}|^2} \right) \right]$$

$E_{implant}$ is the geometry with the implant in the bone, and E_{ref} is the reference case of the bone without the implant.

Chapter 3

3. Simulations and Results

3.1 Geometry

Initially, the geometry consists of the bone in the center with muscle, fat, and skin around it with different widths and parameters [2]. Then, in the second step, we insert an implant inside the bone and perform the simulations. Furthermore, we cover the implant with a bio-compatible Dielectric layer. Another magnetic layer then encapsulates the dielectric layer and to keep the biocompatibility of the structure; we again cover it with a bio-magnetic material. The geometry with an implant and dielectric also simulated for a surface impedance whose response is the same as the initial case. These geometries form five cases mentioned below:

1. Bone, Muscle, Fat, and Skin
2. Implant, Bone, Muscle, Fat, and Skin
3. Implant, Dielectric, Bone, Muscle, Fat, and Skin
4. Implant, Dielectric, Surface Impedance, Bone, Muscle, Fat, and Skin
5. Implant, Dielectric, Magnetic material, Surface Impedance, Bone, Muscle, Fat and Skin

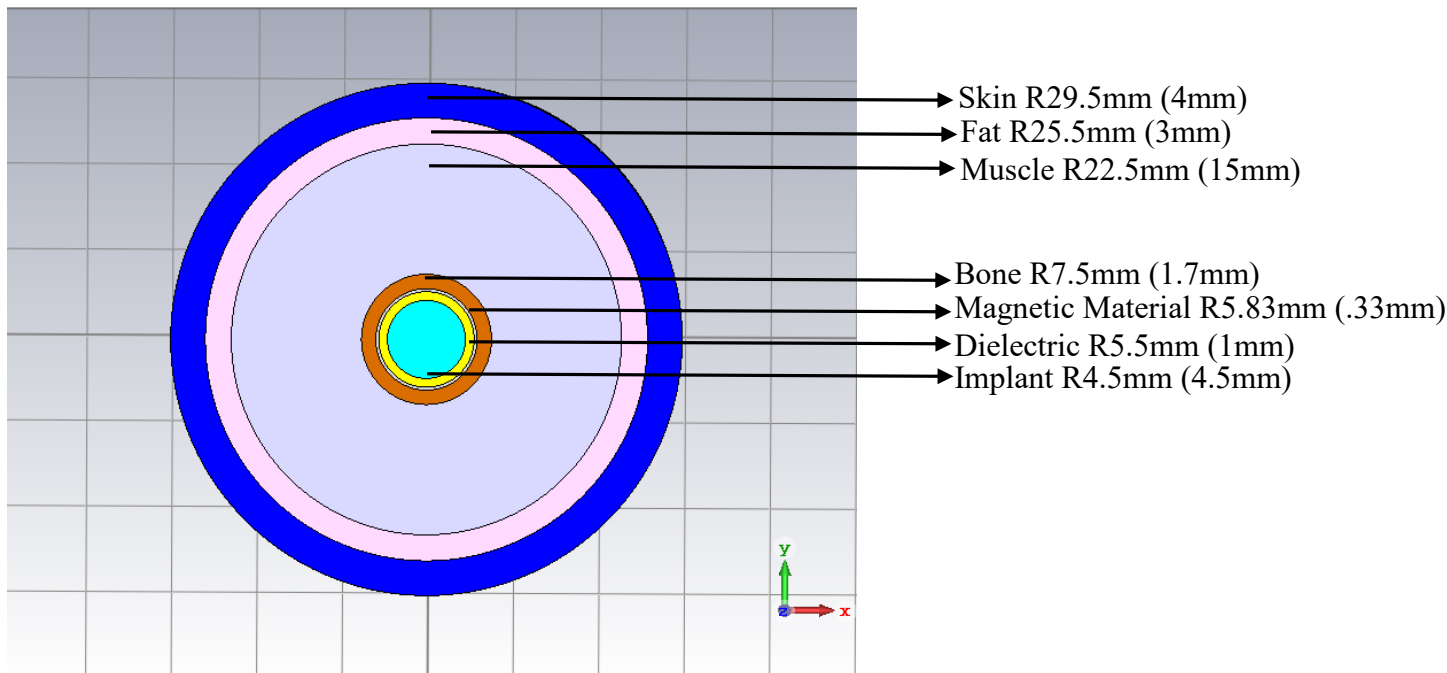


Figure 3: Overview of the complete geometry

3.2 Methodology

The software used for the design and simulation is CST, in which we make use of the microwave studio using periodic structures. The structure is subjected to plane waves from the negative to the positive x-axis, and it is placed perpendicular to the direction of plane waves, i.e., along the z-axis. The response of the plane waves was monitored for every case on the curve placed at the same position inside the bone. The main goal is to achieve the same response of the plane waves in the first case compared to the last case with magnetic material. The curve placed in the bone at 7mm is shown in the following figure.

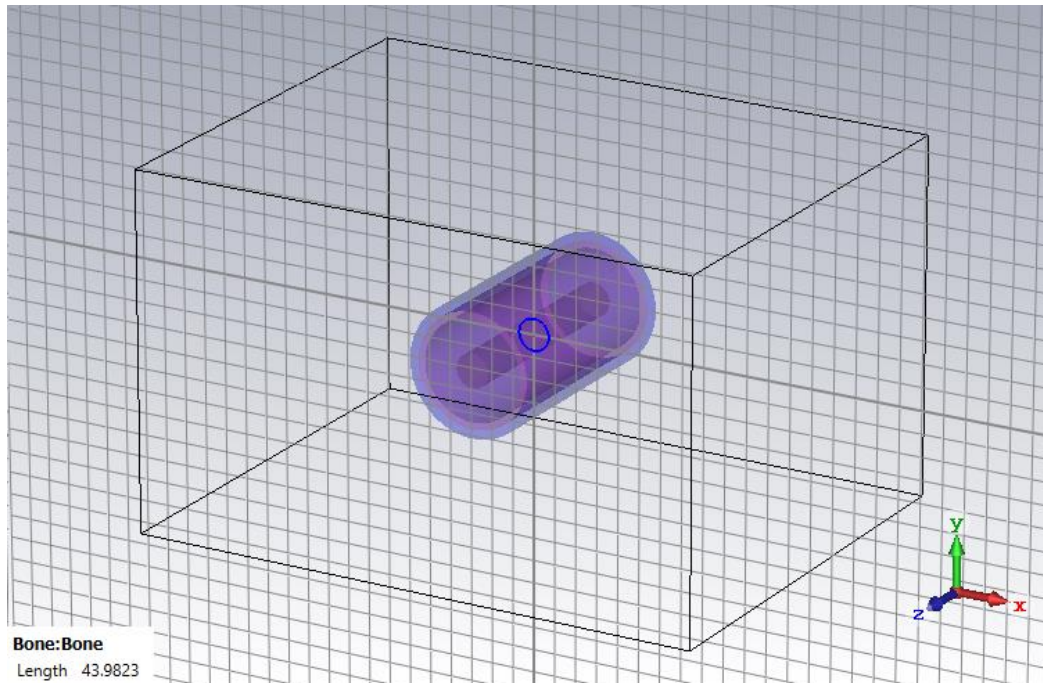


Figure 4: Curve placement inside the bone

All the simulations are performed using three frequencies that are 2.4, 2.45, and 2.5 GHz, but the main focus would be around 2.45 GHz as it is the design frequency. The complete scenario with the model under test and the direction of plane waves is depicted in the figure.

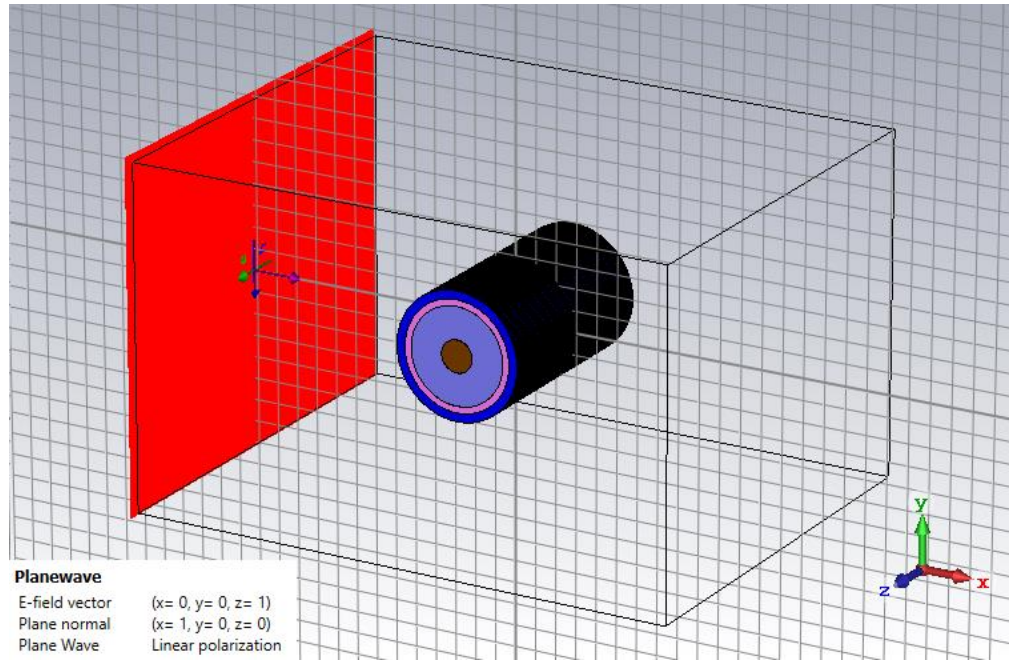


Figure 5: Scenario for the simulation

The boundary conditions for all the axes are kept open (add space), and the background has different spacing like 100 on the lower and higher x-axis, 50 on the lower z-axis, and y-axis.

3.3 Case 1: Bone, Muscle, Fat and Skin

3.3.1 Geometry

The geometry is such that the bone is in the center and muscle, fat, and skin around it with a certain radius, permeability, and conductivity taken from a paper [2] and shown in the following figure.

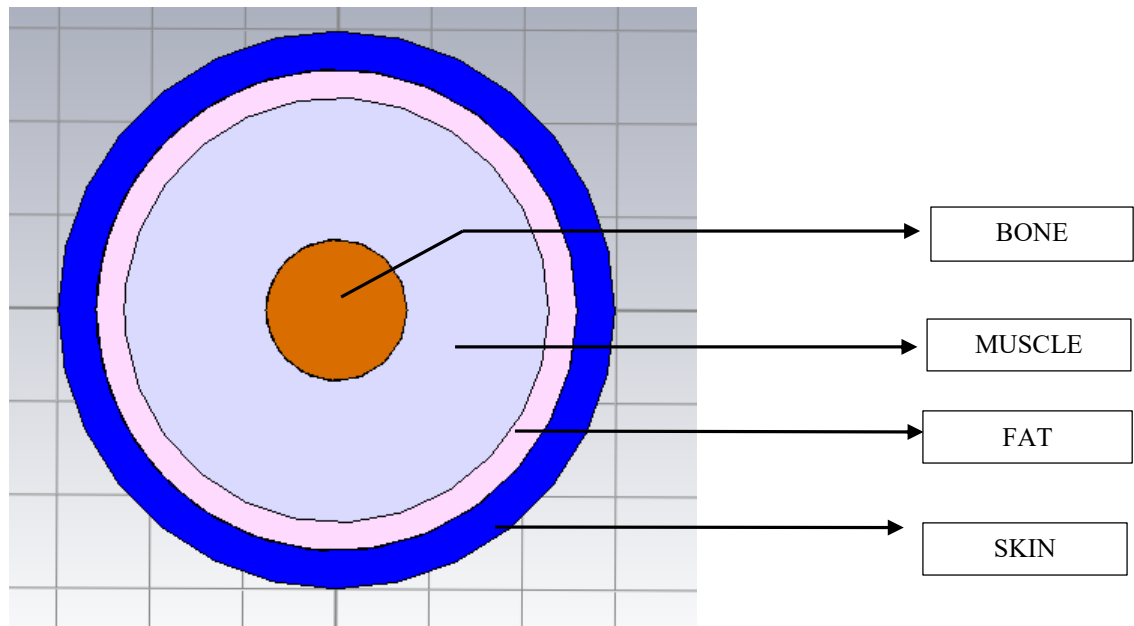


Figure 6: Geometry of only bone structure (case 01)

These parameters are chosen to have fundamental properties to human anatomy and have already been tested in the paper [2].

S. No.	Material	Epsilon	Mu	Conductivity	Radius of material (mm)
1.	Bone	11.207	1	0.4542911	7.5
2.	Muscle	57.1	1	0.79	22.5
3.	Fat	5.56	1	0.04	25.5
4.	Skin	46.7	1	0.69	29.5

Table 1: List of layers and their parameters for case 01

3.3.2 Results

The response of the plane waves should be such that the part of the curve exposed initially should have the maximum intensity of electric field compared to the upper, lower, and back of the curve.

The result at the frequency 2.4 GHz is the same as we expect here we the side lobes are much more and we experience a lower bandwidth of the center peak than 2.45 GHz and 2.5 GHz.

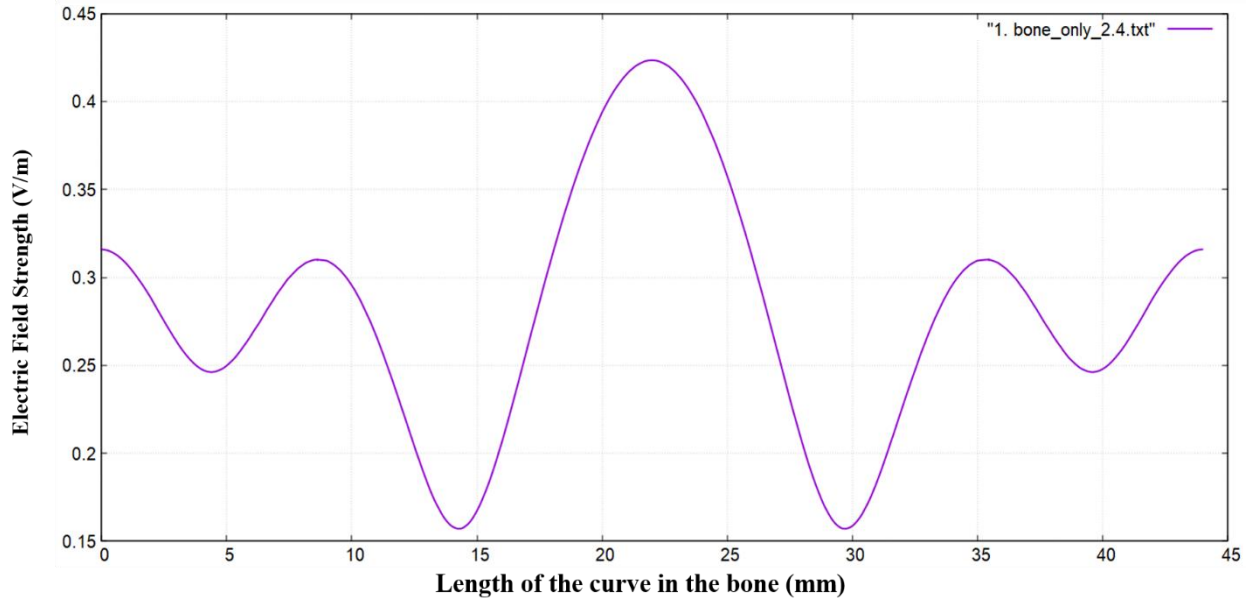


Figure 7: Electric Field Intensity in only bone structure at 2.4 GHz

The design frequency is 2.45 GHz and when we expose the structure at this frequency, we get a better response of electric field intensities along the curve length. The maximum electric field expected and lesser reflections at the sides are visible below the plot with good bandwidth. In this case, as compared to 2.4 GHz, we experience lower sidebands and greater bandwidth.

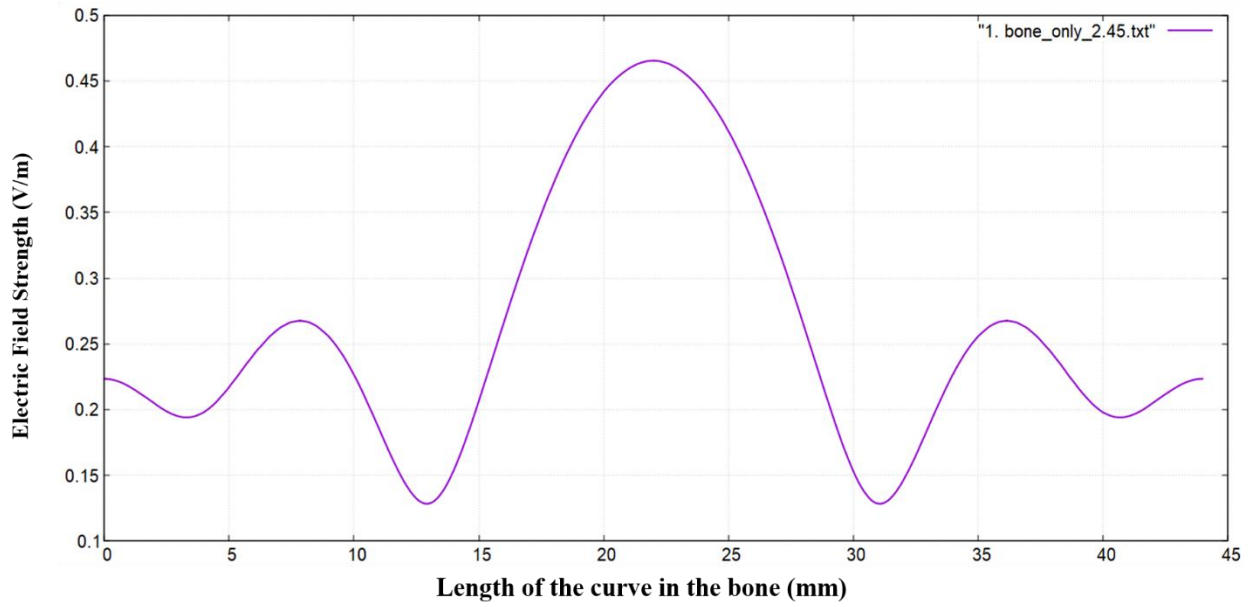


Figure 8: Electric Field Intensity in only bone structure at 2.45 GHz

On the other hand, the response is better at 2.5 GHz than the above two cases as we have more bandwidth and lesser amplitude of sidebands.

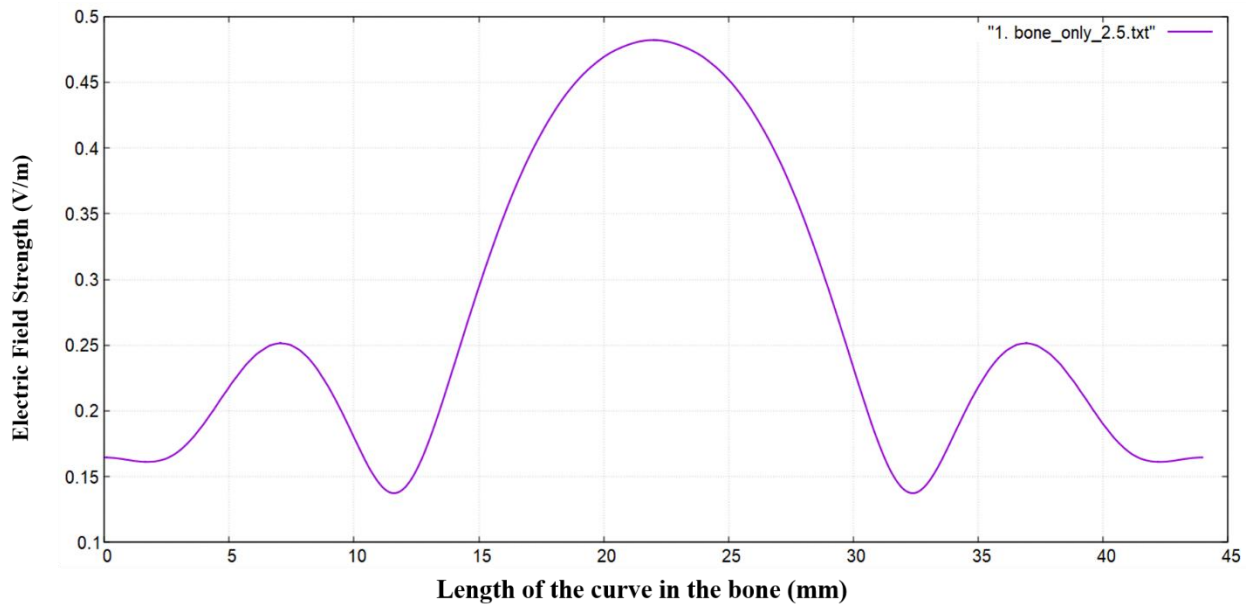


Figure 9: Electric Field Intensity in only bone structure at 2.5 GHz

We considered the case at 2.45GHz as our reference case to compare the results in all further simulations as it is our goal to achieve the same response at the end, plus it is our design frequency.

3.3.3 Comparison

Now we compare the results at the three frequencies just for an overview. The frequency 2.5 GHz performs better as it has more bandwidth, lesser side lobes, and higher amplitude of the central peak. However, our design frequency is 2.45GHz and used for further simulations.

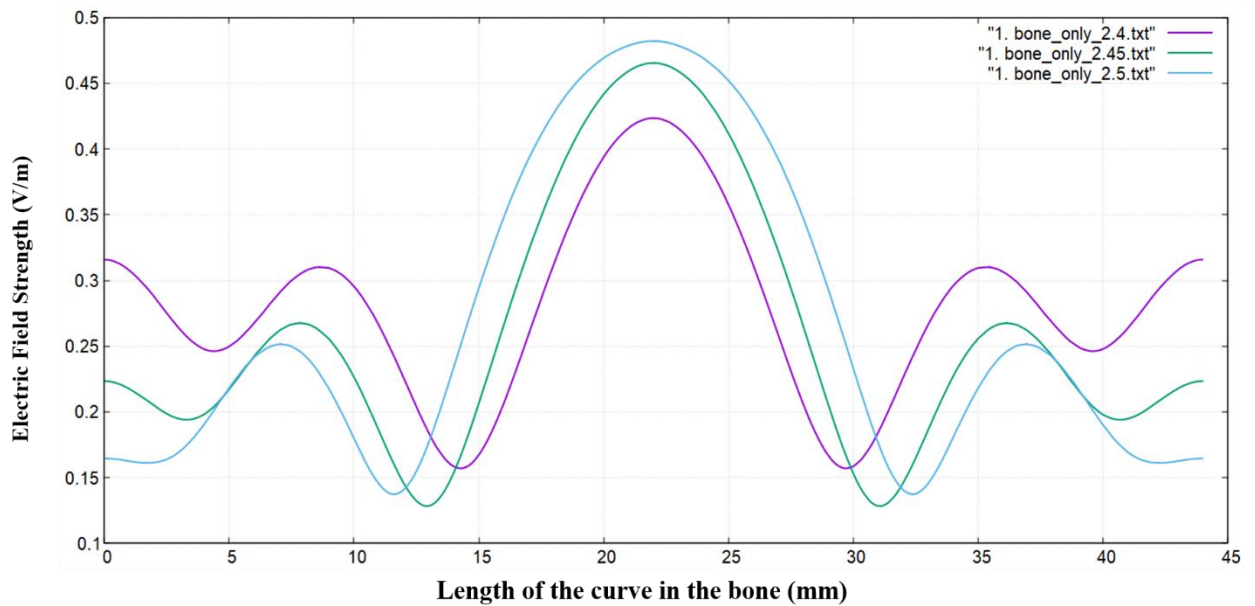


Figure 10: Comparison of Electric Field Intensities at the three frequencies (Case 01)

3.4 Case 2: Implant, Bone, Muscle, Fat, and Skin

3.4.1 Geometry

In this case, we have inserted an implant of 4.5mm inside the bone. The material of the metal used as an implant is Titanium Alloy which is a very commonly used implant.

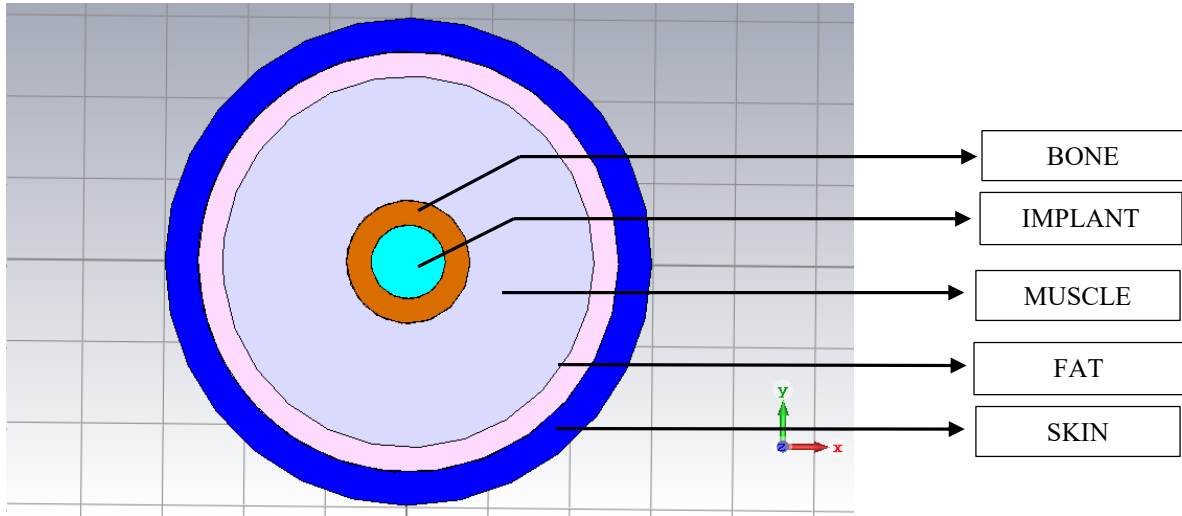


Figure 11: Geometry of bone with implant structure (case 02)

The parameters and the radius are taken from a paper [2], listed below in the table.

S. No.	Material	Epsilon	Mu	Conductivity	Radius of material (mm)
1.	Titanium Alloy (Implant)	-	1	1+e7	4.5
2.	Bone	11.207	1	0.4542911	7.5
3.	Muscle	57.1	1	0.79	22.5
4.	Fat	5.56	1	0.04	25.5
5.	Skin	46.7	1	0.69	29.5

Table 2: List of layers and their parameters for case 02

3.4.2 Results

In the results where we compare the plots for the first and second cases at a particular frequency, we see an apparent degradation in the bandwidth and amplitude of the central peak. The graphs in purple color simulated before adding the implant, and the blue ones show the response for the implantation in the bone.

The plot for the frequency of 2.4GHz shows the response of the implant, which gives less amplitude for the central peak and an increase in the side lobes

amplitude. Here we can observe the reduction in the bandwidth of the central peak as well as well.

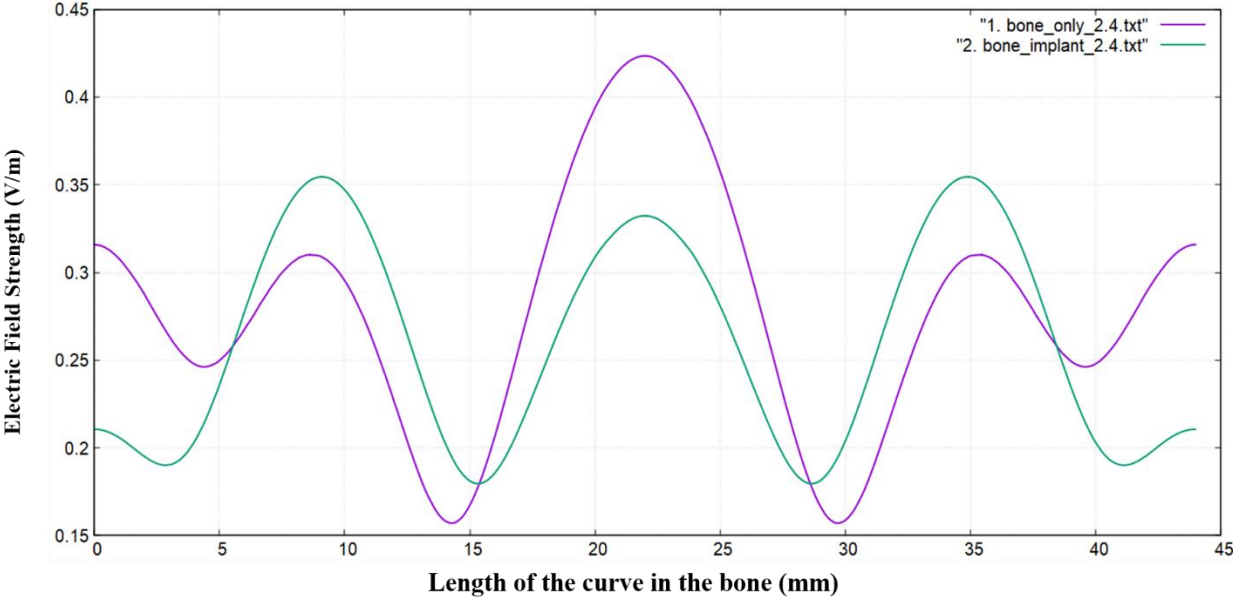


Figure 12: Electric Field Intensity for Bone with Implant at 2.4 GHz

Similarly, for the design frequency, the results have degraded in terms of amplitude and bandwidth.

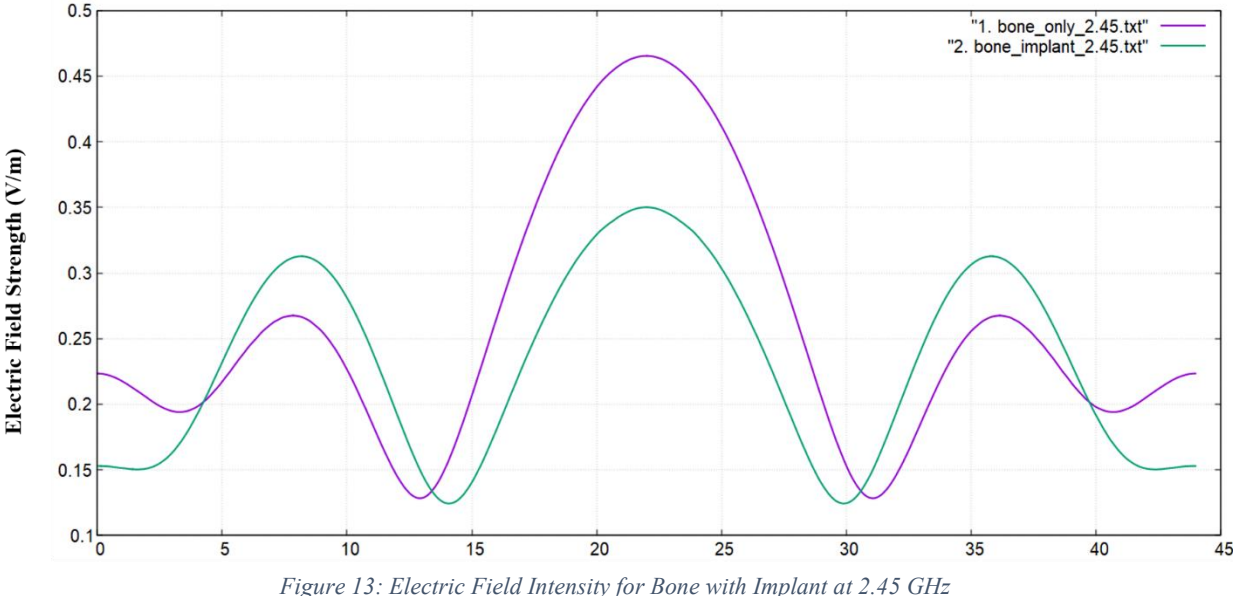


Figure 13: Electric Field Intensity for Bone with Implant at 2.45 GHz

The same behavior is shown by the response at the frequency of 2.5 GHz.

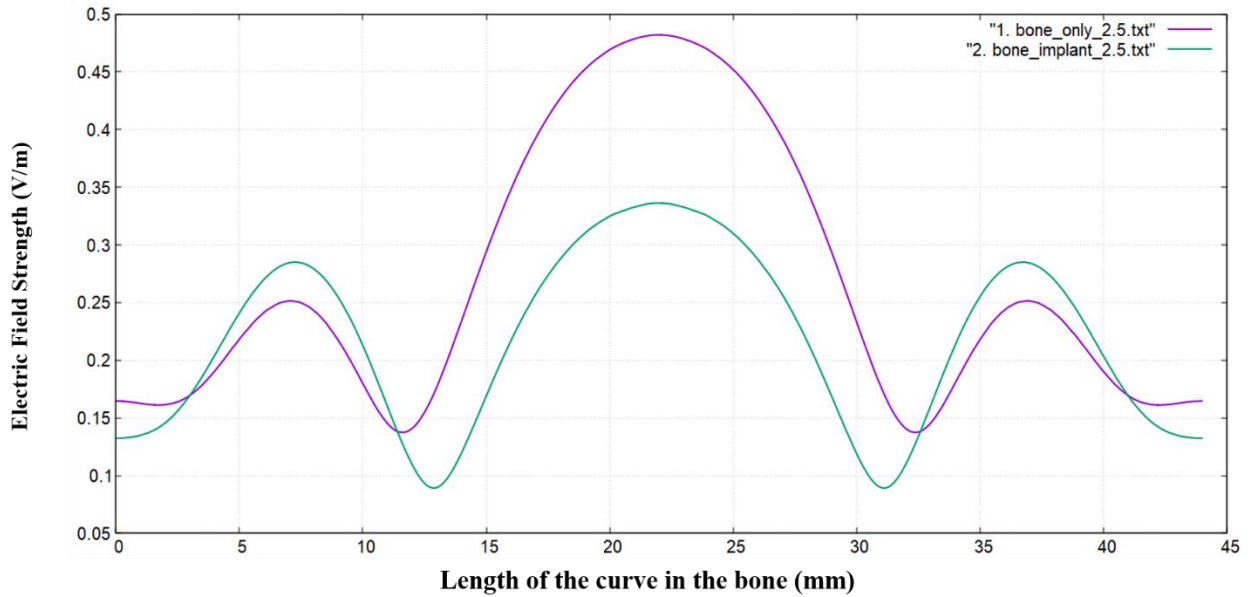


Figure 14: Electric Field Intensity for Bone with Implant at 2.5 GHz

3.4.3 Comparison

We have shown the comparison for the three responses at the frequency mentioned above. Here, the frequency of 2.45GHz performs better in amplitude for the central peak, whereas the frequency 2.5GHz performs better in terms of bandwidth.

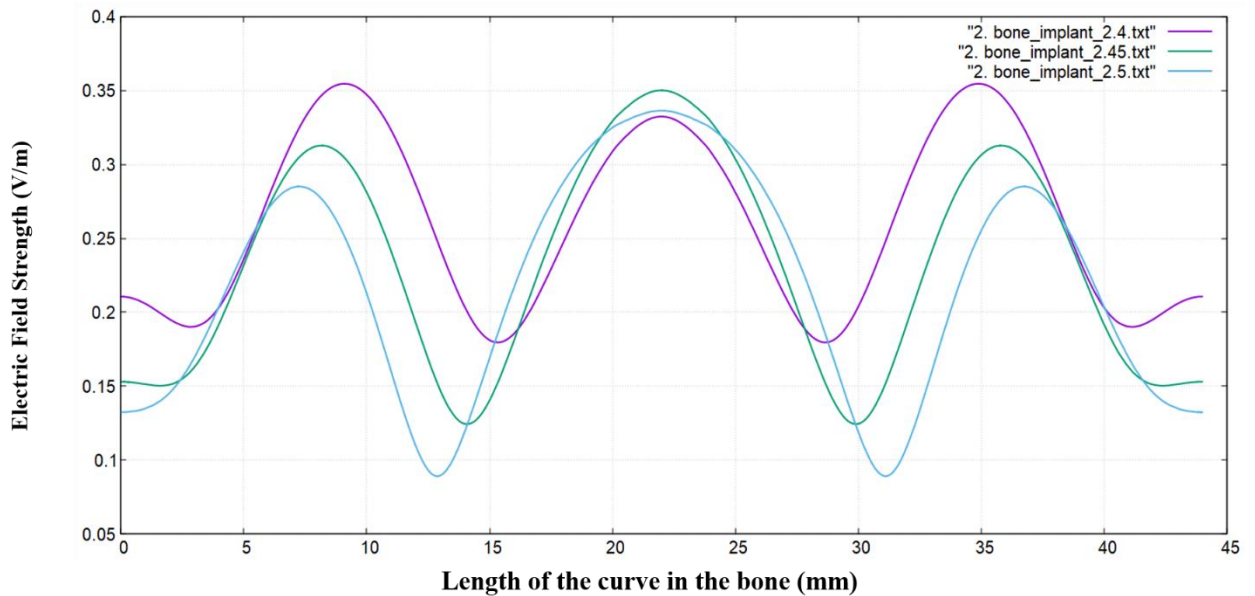


Figure 15: Comparison of Electric Field Intensities at the three frequencies (Case 02)

3.5 Case 3: Implant, Dielectric, Bone, Muscle, Fat, and Skin

3.5.1 Geometry

Now we have added another layer of the dielectric which is the second layer in yellow. We have selected Titanium Dioxide as a biocompatible material to prevent harmful effects of the implant in the long run.

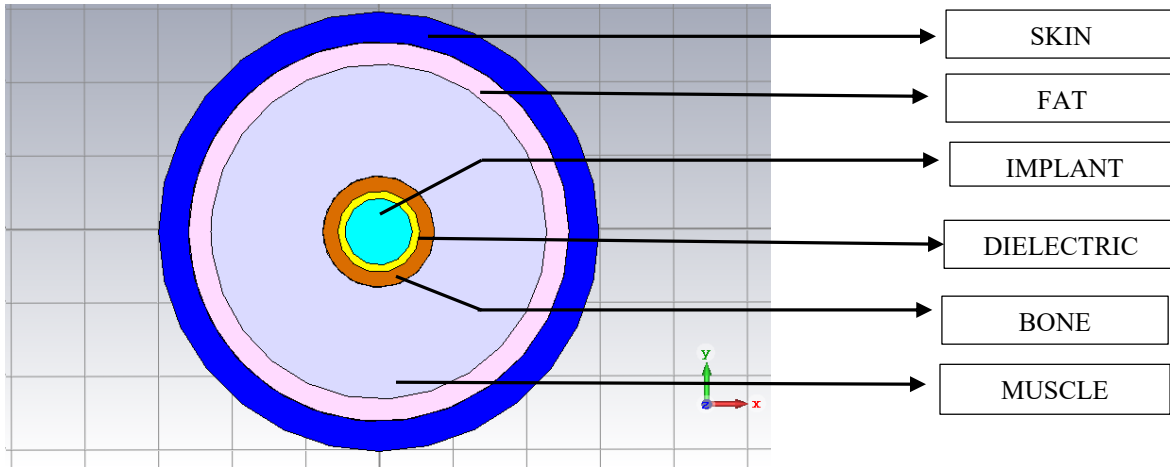


Figure 16: Geometry of Bone, Implant and Dielectric

The parameters and the radius for the above configuration are as follows.

S. No.	Material	Epsilon	Mu	Conductivity	Radius of material (mm)
1.	Titanium Alloy (Implant)	-	1	1+e7	4.5
2.	Dielectric (TiO ₂)	80	1	20	5.5
3.	Bone	11.207	1	0.4542911	7.5
4.	Muscle	57.1	1	0.79	22.5
5.	Fat	5.56	1	0.04	25.5
6.	Skin	46.7	1	0.69	29.5

Table 3: List of layers and their parameters for case 03

3.5.2 Results

We have observed a slight attenuation when adding a dielectric layer compared to the second case when adding only the implant to the bone at all frequencies. The results are shown in the following figures compared to the second case.

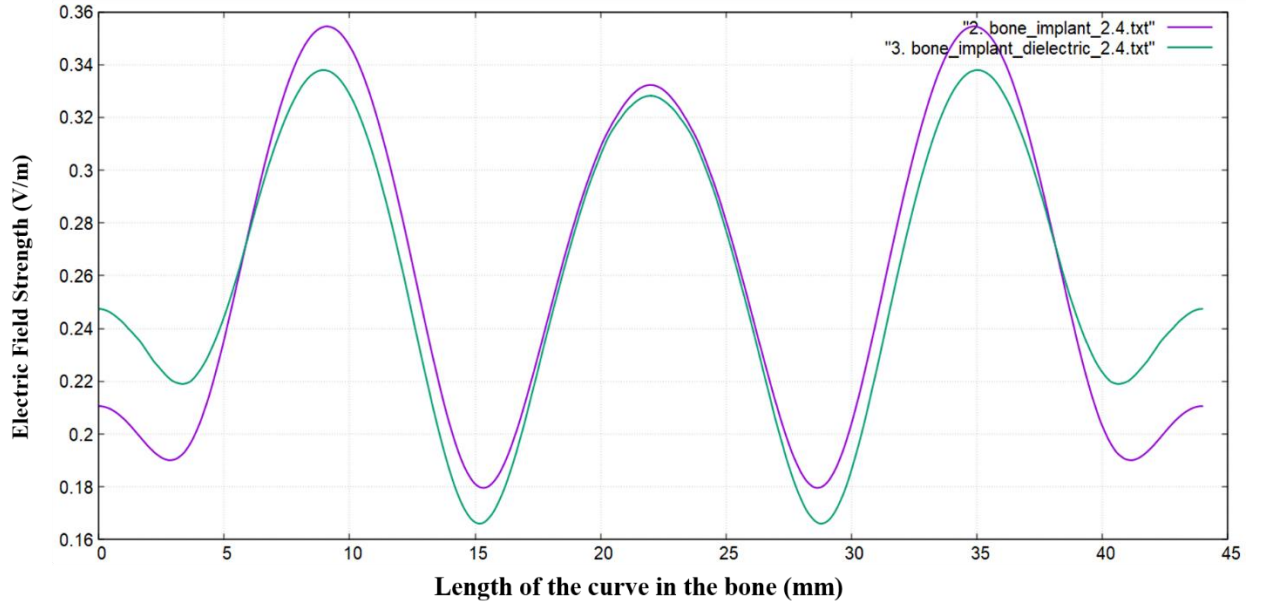


Figure 17: Electric Field Intensity for Bone, Implant and Dielectric at 2.4 GHz

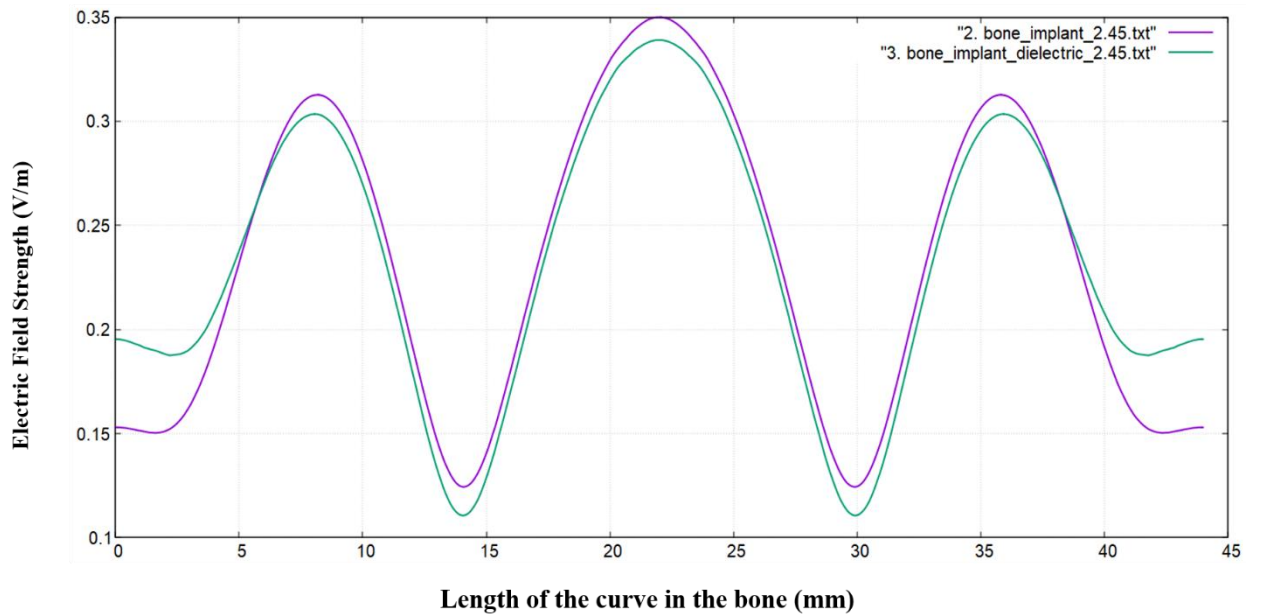


Figure 18: Electric Field Intensity for Bone, Implant and Dielectric at 2.45 GHz

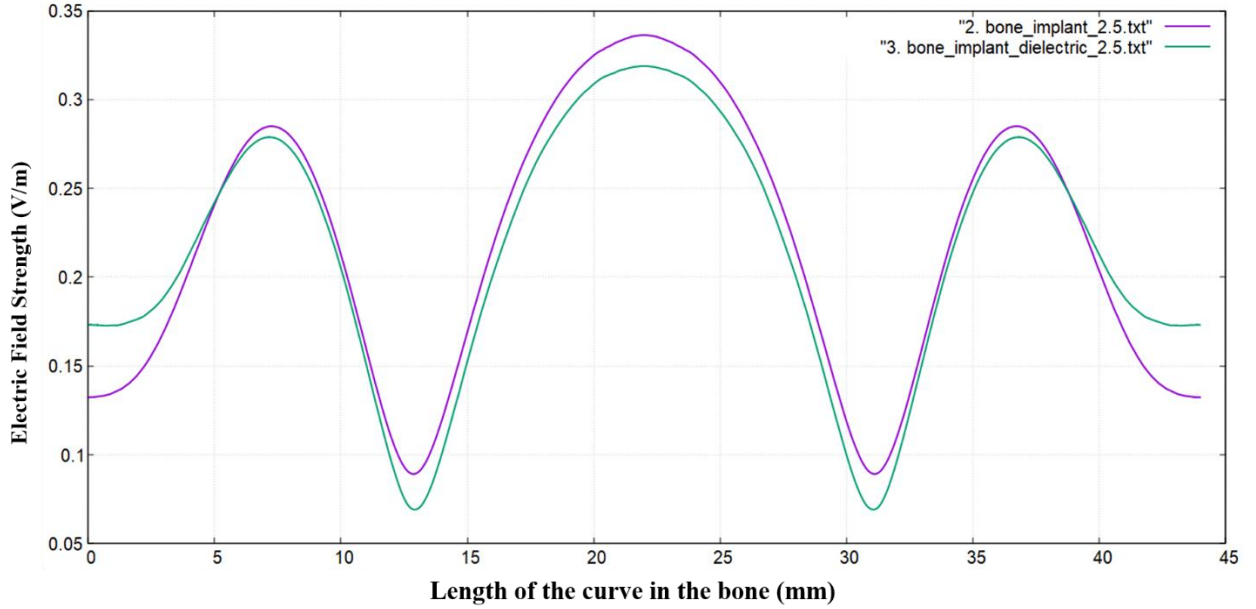


Figure 19: Electric Field Intensity for Bone, Implant and Dielectric at 2.5 GHz

3.5.3. Comparison

We have shown the comparison for the three responses at the frequency mentioned above. Here, the frequency of 2.45GHz performs better in amplitude for the central peak, whereas the frequency 2.5GHz performs better in terms of bandwidth.

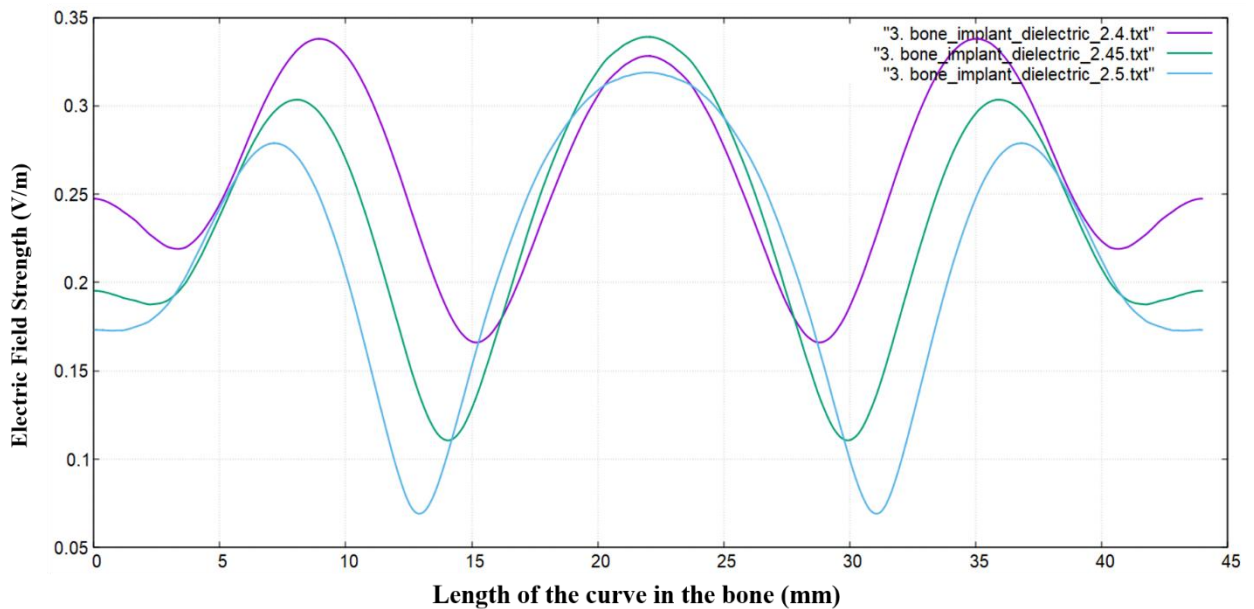


Figure 20: Comparison of Electric Field Intensities of the three frequencies (Case 03)

Now, we compare the case 01, 02 and above structure at the design frequency of 2.45 GHz. We can see degradation in electric field intensity after adding a dielectric layer compared to the second case where we inserted the only implant in the bone.

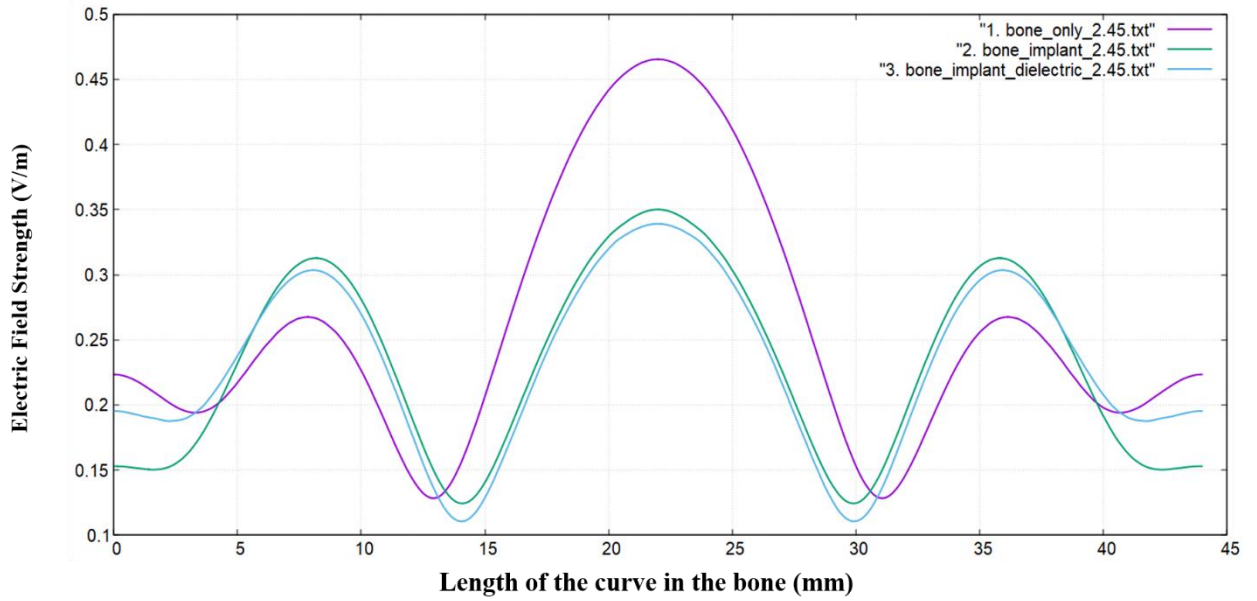


Figure 21: Comparison among Electric Field Intensities of case 01, 02 and 03 at 2.45 GHz

3.6 Case 4: Implant, Dielectric, Magnetic material, Surface Impedance, Bone, Muscle, Fat, and Skin

3.6.1 Geometry

This step identifies the equivalent surface impedance for the third case, which gives a comparable result to the first case by adding a zero thickness negative impedance over the dielectric layer.

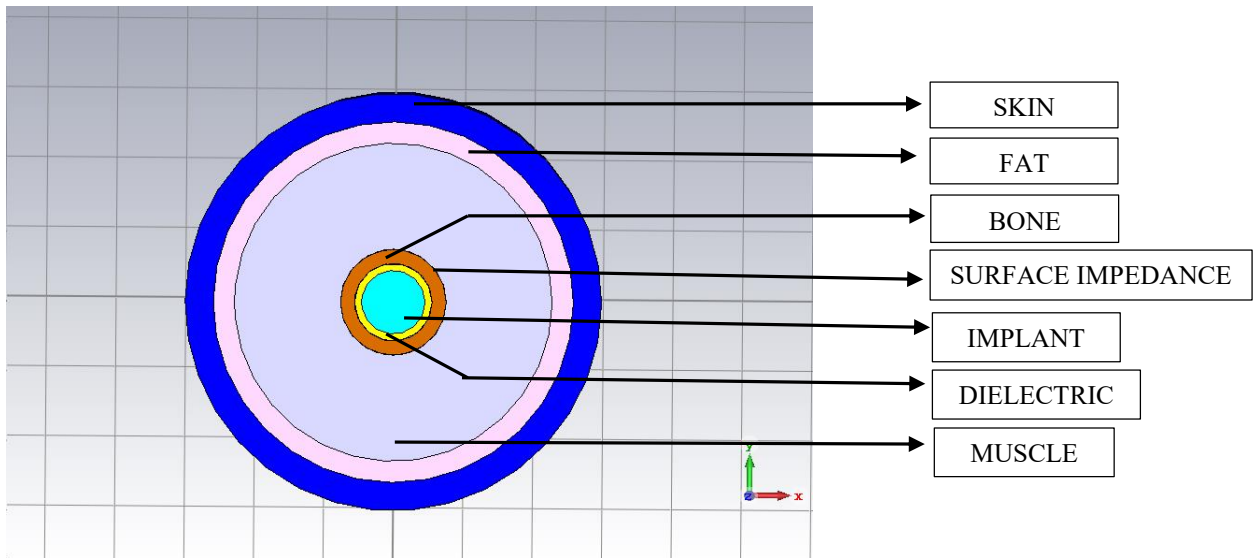


Figure 22: Geometry of the structure after adding surface impedance on the dielectric layer

The parameters and the widths of materials for this case are shown in the table.

S. No.	Material	Epsilon	Mu	Conductivity	Radius of material (mm)
1.	Titanium Alloy (Implant)	-	1	1+e7	4.5
2.	Dielectric (TiO ₂)	80	1	20	5.5
3.	Surface Impedance	-	-	-	-
4.	Bone	11.207	1	0.4542911	7.5
5.	Muscle	57.1	1	0.79	22.5
6.	Fat	5.56	1	0.04	25.5
7.	Skin	46.7	1	0.69	29.5

Table 4: List of layers and their parameters for case 04

3.6.2 Results

The negative imaginary surface impedance was considered starting from $-j10$ Ohm and decreasing until we got a comparable result to the first case with only bone structure. The desired surface impedance was found to be $-j480$ Ohm. These results were computed for all three frequencies.

The results for $-j10$ Ohm illustrated that the results were very degraded when the first sweep was computed and got better with each sweep step until we reached $-j480$ Ohm.

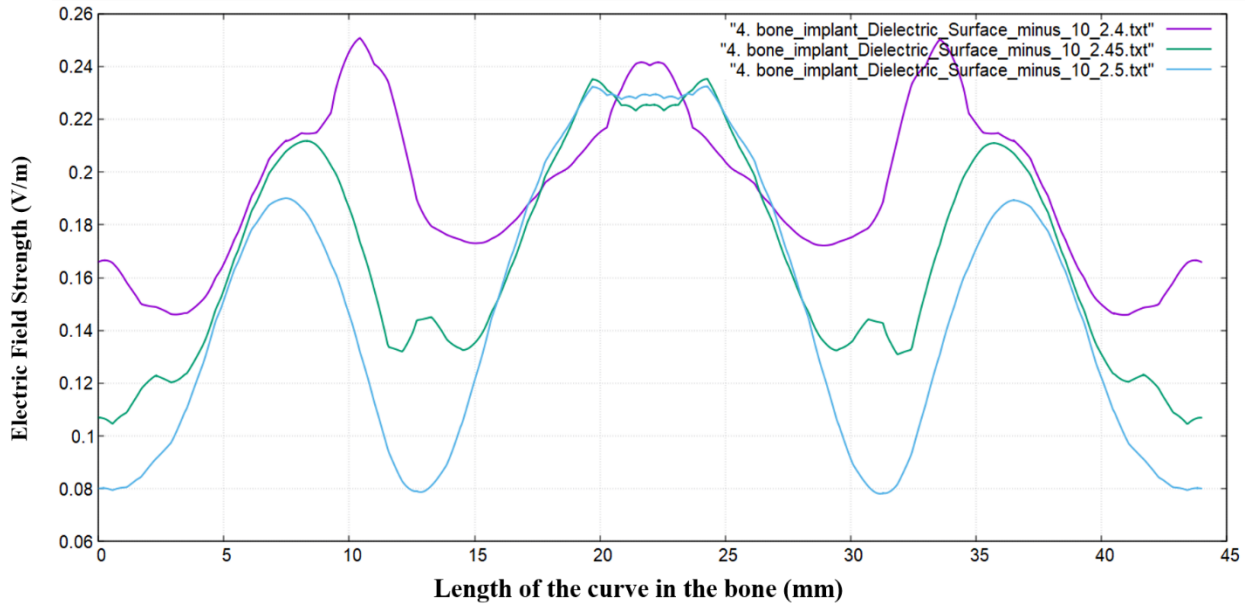


Figure 23: Surface Impedance added to Dielectric Layer of $-j10$ Ohm at the three frequencies

The results for the $-j480$ Ohm is shown below:

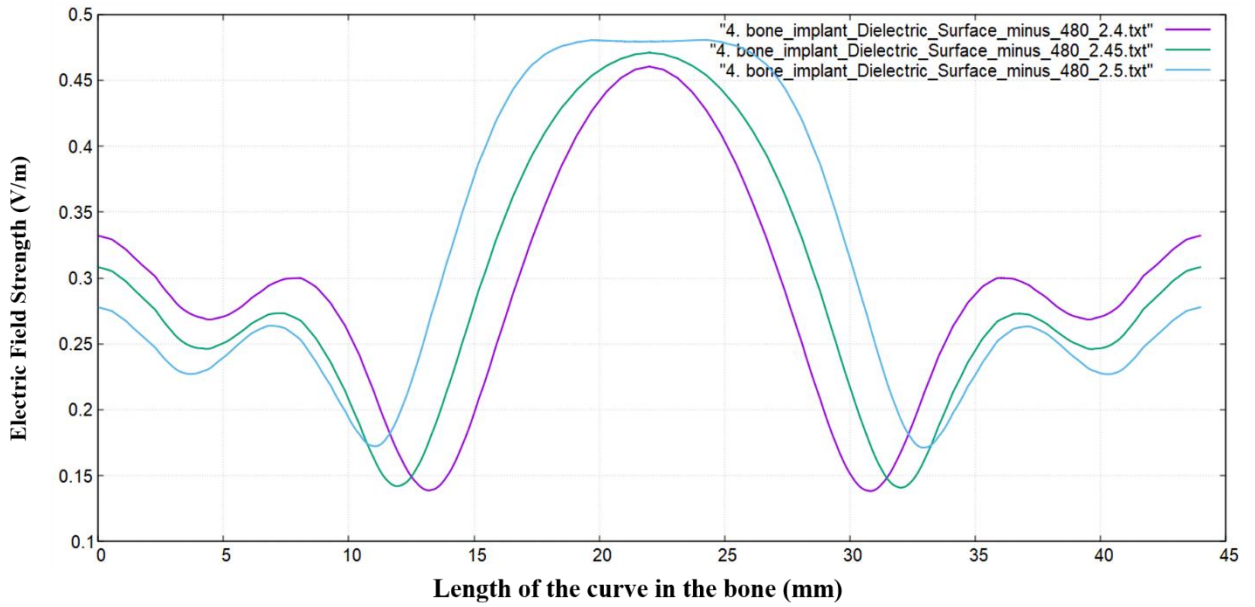


Figure 24: Surface Imp added to Dielectric Layer of $-j480$ Ohm at the three frequencies

3.6.3 Comparison

We need to compare the results for the first and surface impedance cases to assess that the two results for 2.45 GHz are comparable. Looking at the two plots, we have reached very close in terms of amplitude and bandwidth.

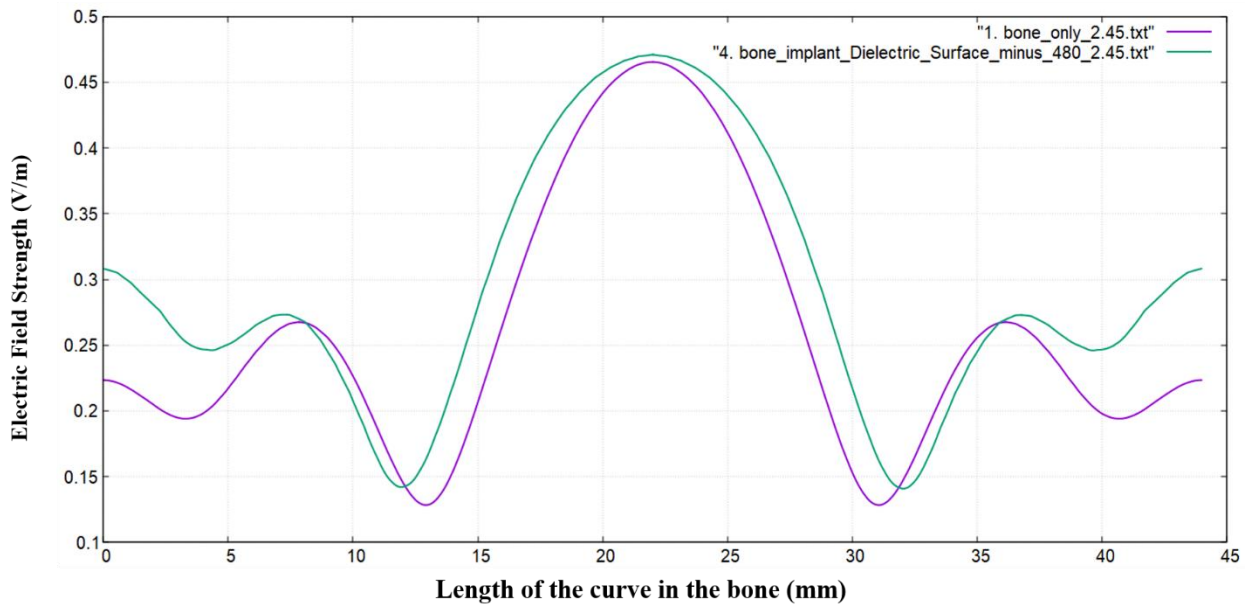


Figure 25: Comparison of only bone case with the surface impedance of -480 Ohm

3.7 Case 5: Implant, Dielectric, Magnetic material, Surface Impedance, Bone, Muscle, Fat, and Skin

3.7.1 Geometry

We remove the surface impedance in the last case and add a new dielectric layer with magnetic material. The magnetic material used here is a lab-developed piezoelectric material that is diamagnetic [3].

Initially, we take the width of this magnetic material as 1mm and reduce it by 0.1mm until we achieve the required response. Then, we reduce or increase the width by 0.01mm for the optimization until we get the best response compared to the bone response in the first case. The geometry is shown in the figure below.

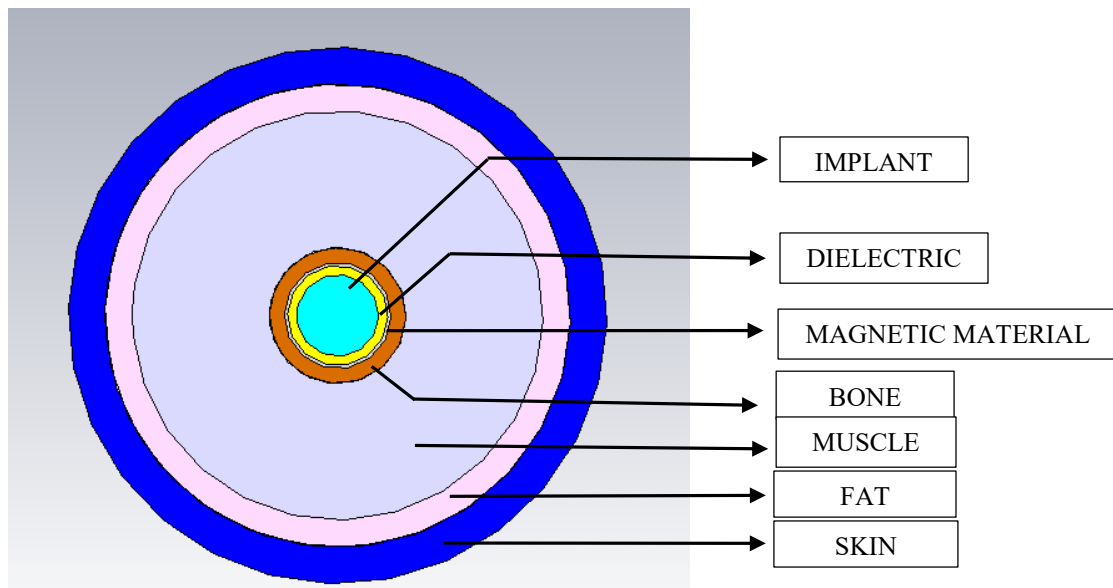


Figure 26: Geometry of the final structure with magnetic material

The number of layers and their parameters are listed below in the following table:

S. No.	Material	Epsilon	Mu	Conductivity	Radius of material (mm)
1.	Titanium Alloy (Implant)	-	1	1+e7	4.5
2.	Dielectric (TiO ₂)	80	1	20	5.5
3.	Magnetic material (PZT)	1028	6e-04	-	5.83
4.	Bone	11.207	1	0.4542911	7.5
5.	Muscle	57.1	1	0.79	22.5
6.	Fat	5.56	1	0.04	25.5
7.	Skin	46.7	1	0.69	29.5

Table 5: List of layers and their parameters for case 05

3.7.2 Results

The plot below is for the frequency 2.4 GHz with an optimized width of magnetic material. Here, the central curve is relatively sharper; it has a lower bandwidth with the side peak much more significant in amplitude than expected.

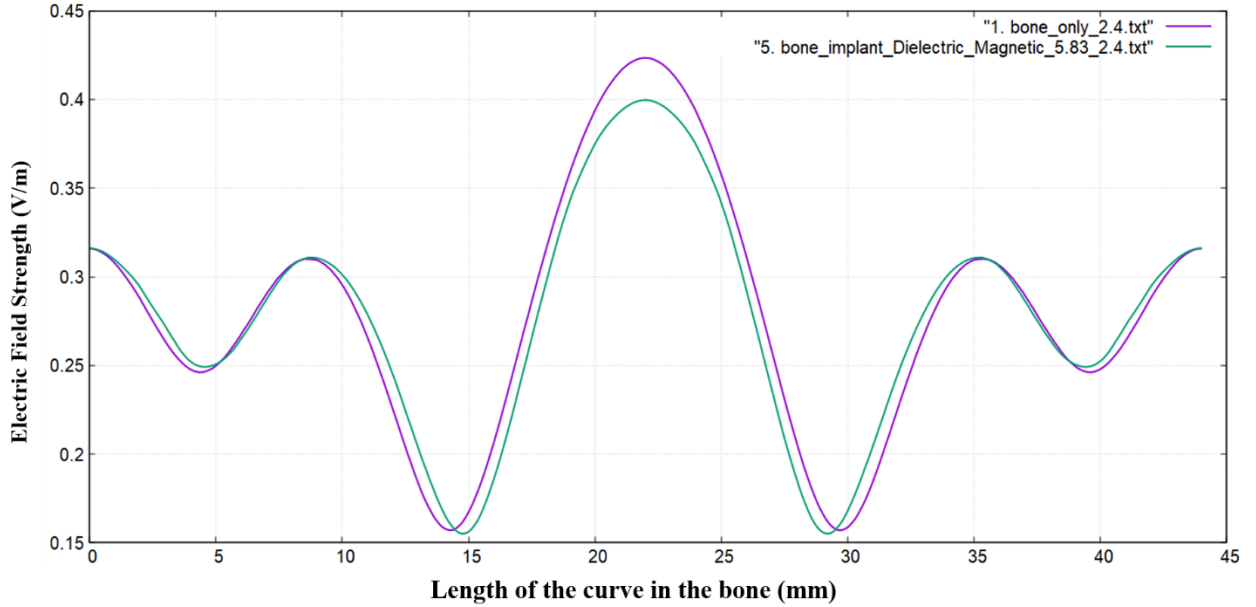


Figure 27: Electric Field Intensity for the final structure with magnetic material at 2.4 GHz

The plot for the frequency 2.45 GHz and the magnetic material has a width of 5.83mm, producing the best response after optimizing the widths. The amplitude and bandwidth are pretty close to the first case of the bone.

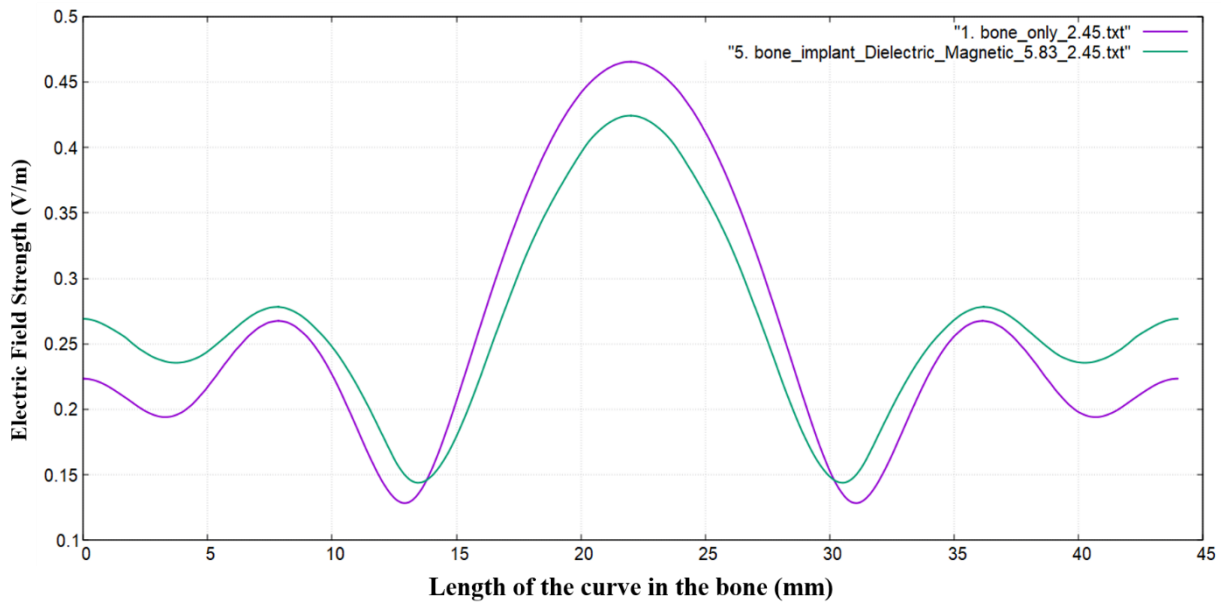


Figure 28: Electric Field Intensity for the final structure with magnetic material at 2.45 GHz

The plot for 2.5 GHz is better among all concerning the amplitude and bandwidth. Also, the amplitude of the side lobes is much less than the above two mentioned frequencies.

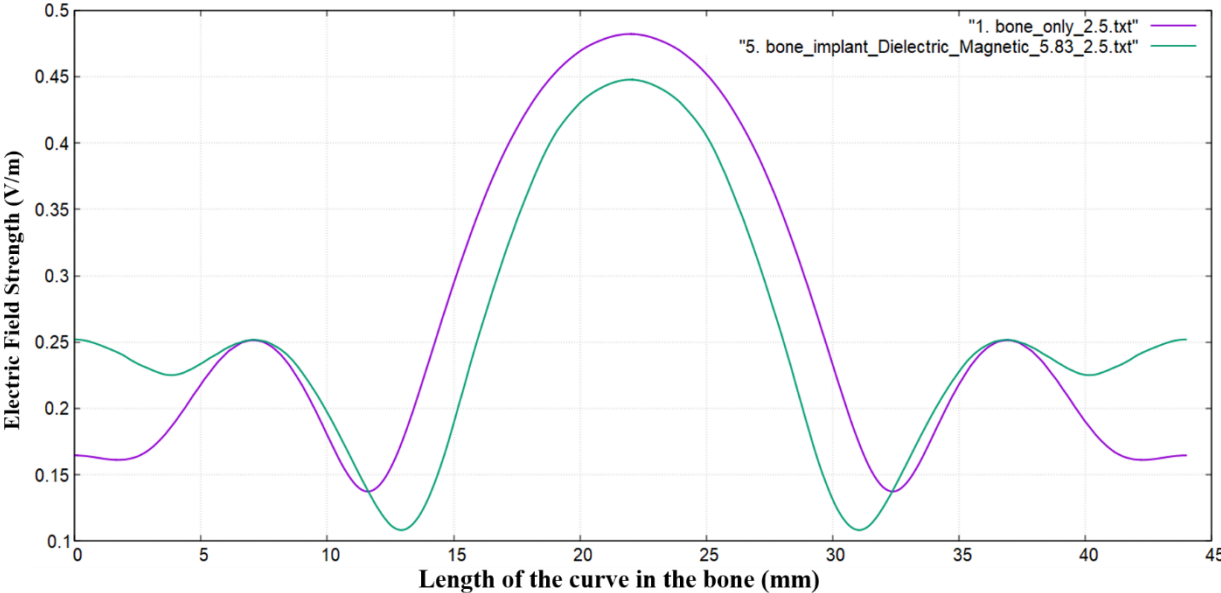


Figure 29: Electric Field Intensity for the final structure with magnetic material at 2.5 GHz

3.7.3 Comparison

We have to make the final comparison between all the cases at our design frequency of 2.5 GHz.

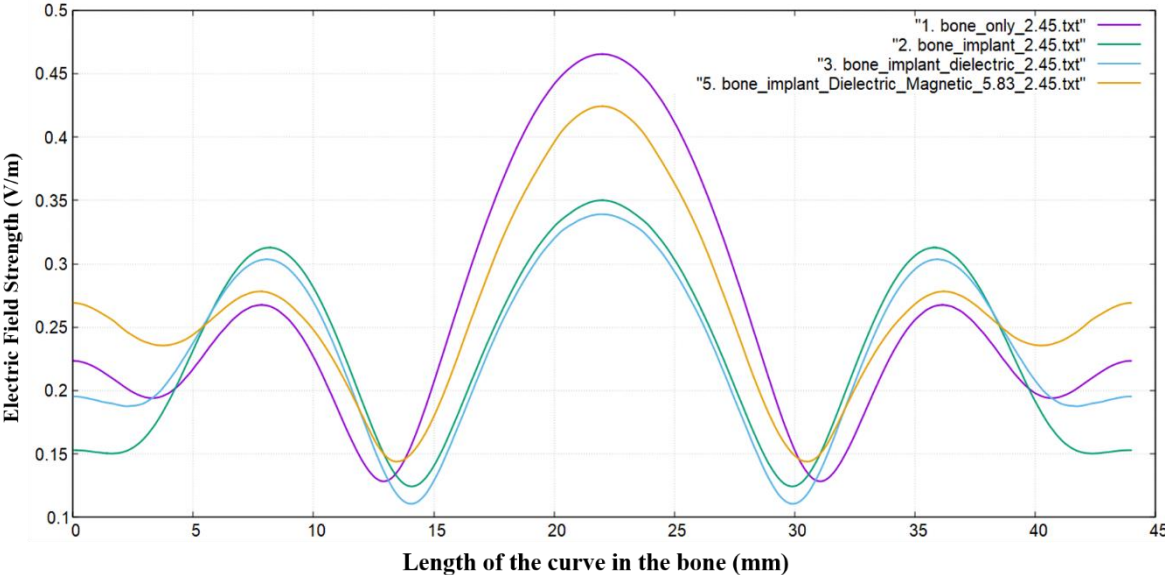


Figure 30: Comparison of all the cases at 2.45 GHz

From the plots above, certainly, an improvement has been made by introducing magnetic material.

Chapter 4

4. Conclusion

To conclude our final results, we have two criteria:

1. Absolute Percentage Error
2. Radar Cross section (RCS)

4.1. Absolute Percentage Error

We calculate two sets of percentage errors for two cases which are:

1. Bone and Implant Case
2. Bone and Magnetic material case

Firstly, we have calculated the percentage error for the bone and implant case.

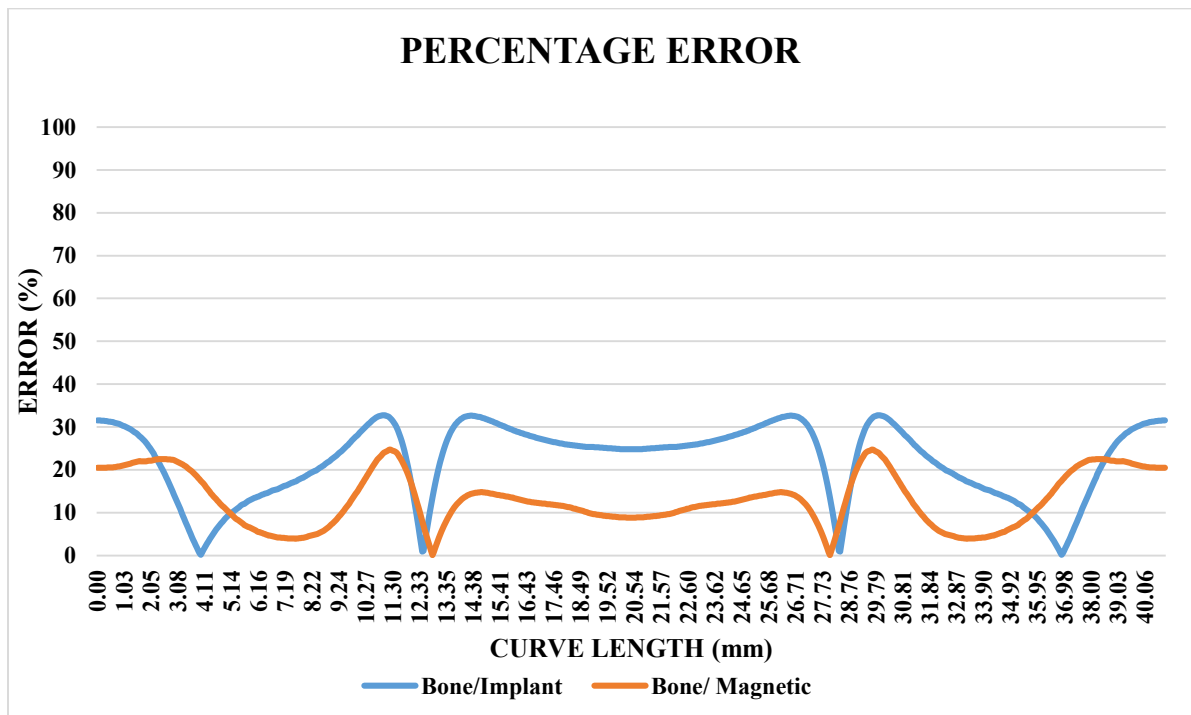


Figure 31: Comparison of Percentage Errors between implant and magnetic material cases

We can see an improvement of error from the implantation to the cloaking from magnetic material. The average error has reduced from 22.2% to 13.08%. So, cloaking from magnetic materials is quite a feasible option here.

4.2. Relative Radar Cross-Section

The relative radar cross-section shows we have reduced the scattering by adding the magnetic material, and it was way too high when we inserted only implant and implant plus dielectric to the bone. In the graph, all zero means no error with respect the initial bone only case.

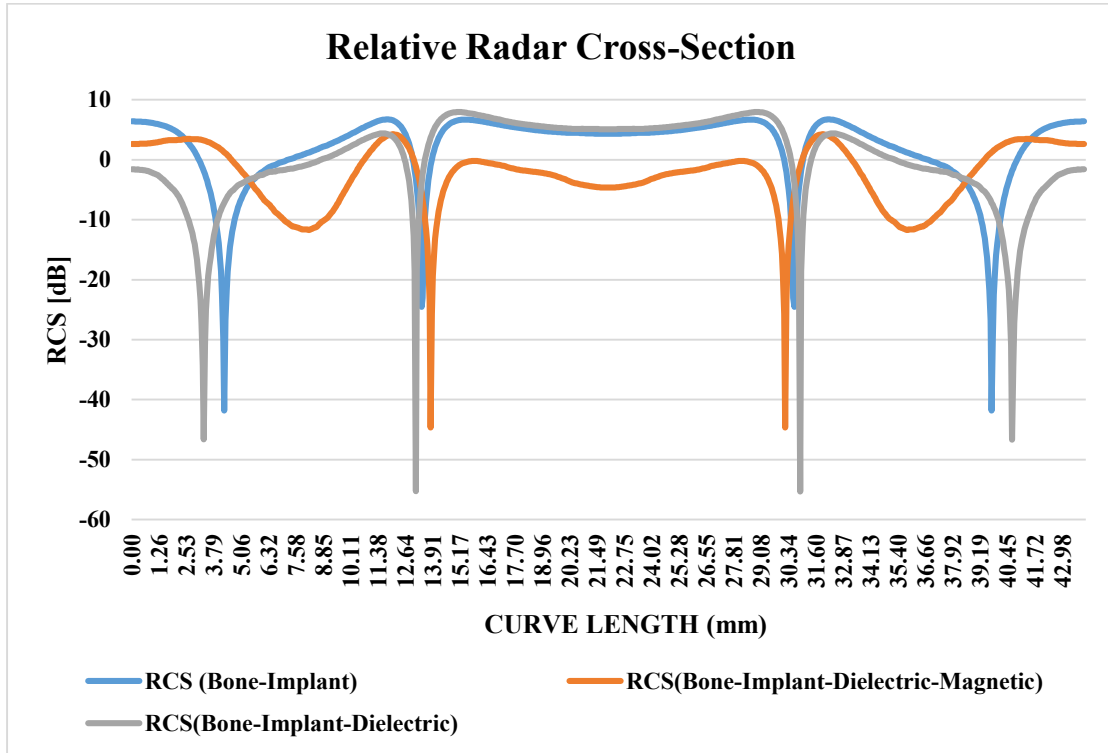


Figure 32: RCS computation for all the cases

4.3 Testing the structure for other values of magnetic permeability

The change in electric field intensity is observed when we change the value of the permeability. The geometry responds in the usual way as the permeability increases; an increase in the value of the electric field strength is observed for the central peak.

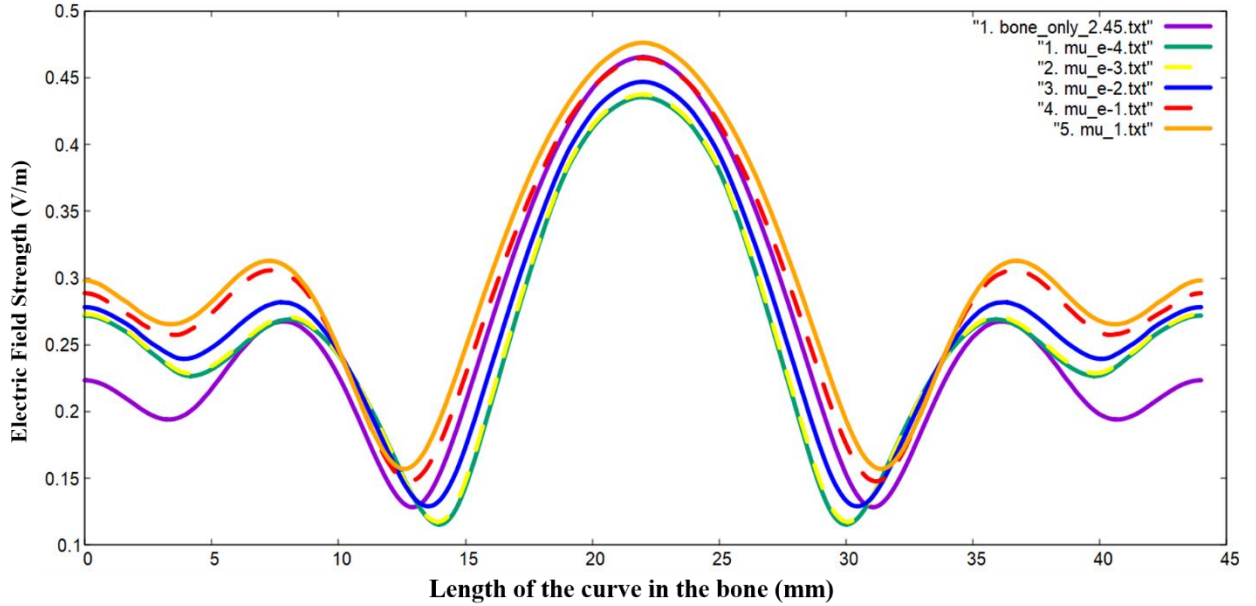


Figure 33: Electric Field Intensities for different values of μ

The results for a μ value equal to $e-01$ give a comparable response to the bone structure, which should give us the least error at the central peak.

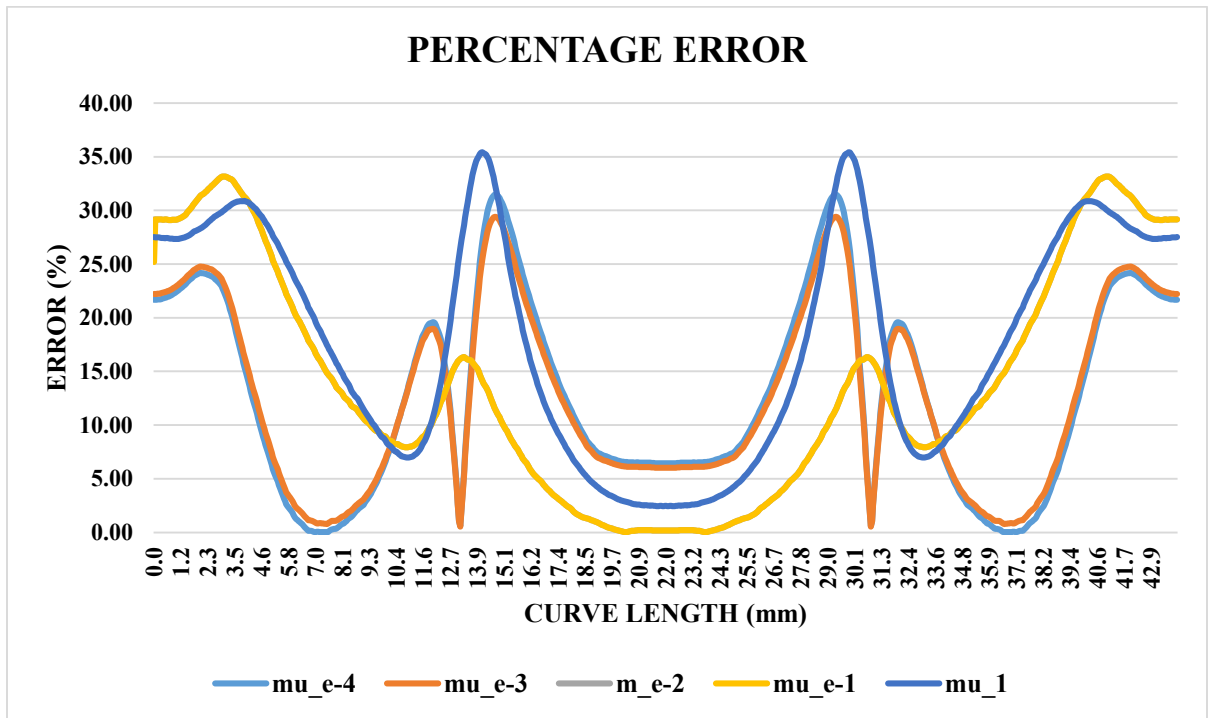


Figure 34: Percentage Errors for different values of μ

References

- [1] <https://statnano.com/news/67822/Polymer-Coating-%E2%80%98Hooks-Up%E2%80%99-Metal-Implants-with-Human-Bones>, Publication date: 13/08/2020, Last visited: 03/12/2021
- [2] L. Matekovits, J. Huang, I. Peter and K. P. Esselle, "Mutual Coupling Reduction Between Implanted Microstrip Antennas on a Cylindrical Bio-Metallic Ground Plane," in *IEEE Access*, vol. 5, pp. 8804-8811, 2017, doi: 10.1109/ACCESS.2017.2703872.
- [3] D. A. Iulia, P. Jana, P. Delia, D. Tudor-Gabriel, L. Matekovits and I. Peter, "Investigation of Multiferroic Properties of Fe^{3+} and $(\text{La}^{3+}, \text{Fe}^{3+})$ doped $\text{PbZr}_{0.53}\text{Ti}_{0.47}\text{O}_3$ Ceramics," *2020 IEEE International Conference on Electrical Engineering and Photonics (EExPolytech)*, 2020, pp. 192-195, doi: 10.1109/EExPolytech50912.2020.9243856.
- [4] L. Matekovits, Y. Su and I. Peter, (2017). On the Radiation Mechanism of Implanted Antennas with Large Conformal Ground Plane. *IET Microwaves, Antennas & Propagation*.11. doi: 10.1049/iet-map.2017.0280.
- [5] G. Labate, S. Podilchak and L. Matekovits. (2017). Closed-form harmonic contrast control with surface impedance coatings for conductive objects. *Applied Optics*. 56. 10055. doi: 10.1364/AO.56.010055.
- [6] B. Cappello and L. Matekovits, "Harmonic analysis and reduction of the scattered field from electrically large cloaked metallic cylinders," *Appl. Opt.* 59, 3742-3750 (2020).
- [7] G. Labate, A. Alù and L. Matekovits. (2017). A Surface Admittance Equivalence Principle for Non-Radiating and Cloaking Problems. *Physical Review A*. 95. 1-6. doi: 10.1103/PhysRevA.95.063841.